Estimation of quantum states by weak and projective measurements

Debmalya Das* and Arvind †

Department of Physical Sciences, Indian Institute of Science Education & Research (IISER), Mohali, Sector-81, SAS Nagar, Manauli P.O. 140306, Punjab, India

(Received 12 March 2014; published 30 June 2014)

We explore the possibility of using "weak" measurements to carry out quantum state tomography via numerical simulations. Given a fixed number of copies of identically prepared states of a qubit, we perform state tomography using weak as well as projective measurements. Due to the collapse of the state after measurement, we cannot reuse the state after a projective measurement. If the coupling strength between the quantum system and the measurement device is made weaker, the disturbance caused to the state can be lowered. This then allows us to reuse the same member of the ensemble for further measurements and thus extract more information from the system. However, this happens at the cost of getting imprecise information from the first measurement. We implement this scheme for a single qubit and show that under certain circumstances, it can outperform the projective measurement-based tomography scheme. This opens up the possibility of new ways of extracting information from quantum ensembles. We study the efficacy of this scheme for different coupling strengths and different ensemble sizes.

DOI: 10.1103/PhysRevA.89.062121 PACS number(s): 03.65.Wj, 03.67.Mn

I. INTRODUCTION

Measurement in quantum physics has a very different connotation as compared to that in classical physics. Measurement invariably disturbs the quantum system, and we say that information comes at a certain cost. The most commonly encountered quantum measurements are projective measurements, wherein the state collapses into one of the eigenvectors of the observable being measured. There is no further information that one can obtain by making a repeated measurement on this collapsed state. Alternatively, one could conceive of "weak" or "unsharp" measurements, where the coupling of the apparatus with the system is weak and only a limited amount of noise is introduced. Consequently, the information obtained from this measurement is also limited. However, there is a possibility of recycling the state and making further measurements on it, which may reveal more information about the state.

Ideal state estimation would require an infinite number of copies of identically prepared states, however, in reality we always have a finite ensemble. Therefore, it would be interesting to explore the possibilities of reducing the size of the ensemble required to achieve a certain amount of fidelity of state estimation. We explore the possibility of carrying out state tomography on finite ensembles using weak measurements, where we recycle the state to extract information about more than one observable. An unsharp or weak measurement is achieved when the apparatus system coupling is weak compared to the initial spread of the pointer state wave functions. This can be achieved by reducing the coupling strength or by preparing the initial pointer states in sufficiently wide wave functions. For such weak measurements the state of the system does not collapse fully, and the state can still be used to extract more information. Such schemes involving weak or unsharp or fuzzy measurements have been proposed in the literature [1–6]. Weak measurement has an interesting property that although it yields very little information [7], the state is correspondingly disturbed very little. However, in such a measurement, the pointer positions corresponding to different eigenvalues of the observer being measured could overlap, leading to an ambiguity. A certain region of the pointer position may therefore have to be discarded in order to reduce the ambiguity in the measurement. Thus we have two parameters, namely, the strength of the measurement and the discard parameter, over which we can optimize the performance of the measurement scheme. This on the one hand provides a novel way of extracting information from a quantum system, and on the other hand, may lead to improvement in fidelity over projective measurements. It may be noted that it is the interplay between the initial state of the pointer and the coupling strength which defines a weak (unsharp) measurement. In fact if we are able to prepare a very narrow initial state of the pointer, even a weak coupling strength can lead to a projective measurement. Weak measurements are also associated with "weak values," which require the notion of postselection [8–11]. This process of postselection leads to throwing away data and can lead to suboptimal use of information from a measurement [12,13]. In our work we use weak or unsharp measurements without postselection. Although all quantum measurements (projective, nonprojective, weak, etc.) can be seen as positive operator valued measures (POVMs), it is important to know the details of a measurement scheme. A POVM can also be interpreted as a projective measurement on a larger Hilbert space [7,14,15]. For a finite ensemble the upper bound on the amount of information extractable is available [16]. The cost of information extraction from quantum systems in terms of disturbance caused has also been explored in the context of weak measurements [17–19].

A good way to represent pure as well as mixed states of a single qubit is to use the Bloch sphere [14,20]. The Bloch sphere is a unit ball and every point on and inside the sphere represents a quantum state of the qubit. The state corresponding to the point (x,y,z) is given by

$$\rho = \tfrac{1}{2}(I + \vec{n}\cdot\vec{\sigma}), \tag{1}$$

*debmalya@iisermohali.ac.in
†arvind@iisermohali.ac.in

 ©2014 American Physical Society

where $\hat{n} = x\hat{x} + y\hat{y} + z\hat{z}$ is a vector with $x = \langle\sigma_x\rangle$, $y = \langle\sigma_y\rangle$, and $z = \langle\sigma_z\rangle$. The pure states correspond to the case when the point lies on the surface and in that case $\vec{n}$ is a unit vector. The expectation values of σ_x, σ_y, and σ_z serve as a direct means to calculate the values of (x,y,z). Therefore, to carry out state estimation of a given state of a single qubit, we need to estimate the numbers (x,y,z).

The efficacy of any state tomography procedure is determined by the closeness of the estimated state to the state being tomographed. This requires an appropriate fidelity measure. Since we are dealing with general states of a qubit we consider the distance between the estimated state and the original state on the Bloch sphere as a measure of the fidelity of the tomography scheme. Let us assume that the estimated values of (x,y,z) are $(x_{\text{est}},y_{\text{est}},z_{\text{est}})$ for a given estimation scheme. We define a measure of fidelity as

$$f = 1 - [(x - x_{\text{est}})^2 + (y - y_{\text{est}})^2 + (z - z_{\text{est}})^2] \tag{2}$$

The fidelity is a measure of the distance between the original state and the estimated state. For a perfect estimation f is equal to 1. The amount by which f is less than 1 measures the departure of the estimate from the original state. We will use this measure throughout this paper to measure the efficacy of the state estimation schemes.

This work explores state reconstruction for pure and mixed states of a qubit using weak measurements and compares the efficacy of this scheme with that using projective measurements. Since state tomography requires an ensemble of identically prepared states, we have assumed finite ensembles and calculated the dependence of the fidelity of the tomography scheme as a function of ensemble size in both cases. We show that under certain circumstances, weak measurements with state recycling can be a better tool for state reconstruction. This we believe extends the scope of extracting information from quantum systems at a reduced cost.

The material in this paper is arranged as follows. In Sec. II we describe weak measurements. Section III details the tomography procedure using weak measurements on finite ensembles. In this section the main results of the simulation are presented. Section IV contains some discussion and concluding remarks.

II. WEAK MEASUREMENTS IN QUANTUM MECHANICS

The process of gaining information from a quantum system typically requires an apparatus with distinct classical (macroscopic) pointer positions to interact with the quantum system followed by a readout of the pointer positions. A useful model of this process is available due to von Neumann. Although originally this model was constructed for strong (projective) measurements [21] it has wider applications and can also be applied to weak measurements [1–6,8,9].

Consider the measurement of an observable A of a quantum system with eigenvectors $\{|a_j\rangle\}$ and eigenvalues $\{a_j\}$, $j = 1,\ldots,n$. Imagine an apparatus with continuous pointer positions described by a variable q and its conjugate variable p such that $[q,p] = i$. The initial state of the measuring device has an initial spread of Δq with its initial Gaussian quantum state $|\phi_{\text{in}}\rangle$ centered around zero given by

$$|\phi_{\text{in}}\rangle = \left(\frac{\kappa}{2\pi}\right)^{\frac{1}{4}} \int_{-\infty}^{\infty} dq\, e^{-\frac{\kappa q^2}{4}} |q\rangle, \tag{3}$$

where $\kappa = \frac{1}{(\Delta q)^2}$ and we have taken $\hbar = 1$. The system and the measuring device are made to interact by means of a Hamiltonian,

$$H = g\delta(t - t')A \otimes p, \tag{4}$$

where p is the momentum conjugate to the variable q, and g is the coupling strength. The Hamiltonian is so chosen that the system and the device get a kick and interact momentarily at $t = t'$. Let the initial state $|\psi_{\text{in}}\rangle$ of the system be written in terms of the eigenstates $|a_1\rangle,|a_2\rangle,\ldots,|a_n\rangle$ of the operator A:

$$|\psi_{\text{in}}\rangle = \sum_{i=1}^{n} c_i |a_i\rangle. \tag{5}$$

The joint evolution of the system and the measuring device under the coupling Hamiltonian gives an entangled state for $t > t'$:

$$e^{-i\int H dt}|\psi_{\text{in}}\rangle \otimes |\phi_{\text{in}}\rangle = \left(\frac{\kappa}{2\pi}\right)^{\frac{1}{4}} \sum_{i=1}^{n} \int_{-\infty}^{\infty} dq c_i\, e^{-\frac{\kappa(q-ga_i)^2}{4}} |a_i\rangle \otimes |q\rangle. \tag{6}$$

The above state consists of a series of Gaussians centered at $ga_1,ga_2,\ldots,ga_n$ for the pointer entangled with corresponding eigenstates $|a_1\rangle,|a_2\rangle,\ldots,|a_n\rangle$ of the system. At this stage we invoke the "classicality" of the apparatus, because of the fact that only one of the pointer positions actually shows up. This requires the collapse of the wave function which is brought in as something natural for the classical apparatus. Thus the process is completed with the meter showing only one of the ga_is. Consequently, the system state collapses into the corresponding eigenstate $|a_i\rangle$. The above analysis holds good only if the Gaussians are well separated or distinct. In case they overlap, which can happen if the coupling strength g is small or the initial spread in the pointer state given by $1/\kappa$ is large, the scenario changes [1,8,22]. This is called the weak or unsharp measurement regime. Weak measurements have been employed in developing recipes for the violation of Bell inequalities [22] and Leggett Garg inequalities [23]. These have also been recently used to study super quantum discord [24,25].

In the treatment of weak measurement given by Aharonov, Albert, and Vaidmann (AAV), a subsequent projective measurement of a second observable is carried out, followed by a postselection of the output state into one of the eigenstates of the second observable. However, we take a different approach in our work, where we do not do any postselection; i.e., we consider *weak measurements without weak values*.

How exactly do we carry out the weak measurement? How much is the effect of a weak measurement on the system? If we carry out weak measurements on all the members of an identically prepared ensemble, what happens to such an ensemble? We illustrate these points by taking an example. Consider a measurement of σ_z (z component of spin) of a qubit in a fixed quantum state. Following the general prescription

given in Eq. (4) we write the interaction Hamiltonian

$$H = g\delta(t - t')\sigma_z \otimes p \tag{7}$$

assuming the initial state of the pointer to be the same as that given in Eq. (3). The qubit is taken to be in a pure state given by

$$|\psi_{\text{in}}\rangle = \cos\frac{\alpha}{2}|0\rangle + \sin\frac{\alpha}{2}|1\rangle, \tag{8}$$

where $|0\rangle$ and $|1\rangle$ are the eigenstates of σ_z with eigenvalues $+1$ and -1, respectively. The combined state of the system and the pointer after the interaction is given by taking a special case of Eq. (6):

$$|\psi_{\text{out}}\rangle = \left(\frac{\kappa}{2\pi}\right)^{\frac{1}{4}} \int_{-\infty}^{\infty} dq \cos\frac{\alpha}{2}\, e^{-\frac{\kappa(q-g)^2}{4}} |0\rangle \otimes |q\rangle + \left(\frac{\kappa}{2\pi}\right)^{\frac{1}{4}} \int_{-\infty}^{\infty} dq \sin\frac{\alpha}{2}\, e^{-\frac{\kappa(q+g)^2}{4}} |1\rangle \otimes |q\rangle. \tag{9}$$

At this stage the apparatus and the system are in an entangled state. An observation of the apparatus will lead to values whose distribution is determined by the above state. It is clear from Eq. (9) that the distribution of values of the apparatus is a Gaussian centered around $+g$ for the system input state $|0\rangle$ and is a Gaussian centered around $-g$ for the system input state $|1\rangle$. The width of the Gaussian in each case is given by $1/\kappa$. By tuning the parameter $\epsilon = \kappa g$ we can change the nature of the measurement in terms of its strength. In our work we have taken $g = 1$ so that we have $\epsilon = \kappa$. For large values of ϵ we have a projective measurement, where the pointer distributions are well separated for the states $|0\rangle$ and $|1\rangle$. Therefore, each reading of the pointer tells us exactly what the state of the system is after the measurement. By repeatedly measuring the same observable we can calculate the expectation value of the observable. The state collapses completely in each measurement and there is no question of reusing these states. However, when the value of ϵ is small we have two Gaussians that overlap. From an observation of the pointer we do not learn with certainty as to what value to assign to the system spin z component. The pointer positions are weakly correlated with the eigenstates of σ_z. The state is only partially affected and there is a possibility of reusing the state. The effect of the weak measurement in this case can be explicitly calculated and it turns out that there is very little change in the state of the system. The final state of the system can be calculated by taking the state in Eq. (6) and then taking a partial trace over the apparatus's degrees of freedom giving us the final mixed state corresponding to the system alone:

$$\rho_f = \frac{1}{2}\begin{pmatrix} 1 + \cos\alpha & \left(1 - \frac{\epsilon}{8}\right)\sin\alpha \\ \left(1 - \frac{\epsilon}{8}\right)\sin\alpha & 1 - \cos\alpha \end{pmatrix}. \tag{10}$$

Since ϵ is small we can conclude that the disturbance caused to the system is also small. Furthermore, the disturbance can be controlled by changing ϵ.

A recent work by Rozema *et al.* suggests some new possibilities that weak measurements can offer with respect to Heisenberg's uncertainty relation and the disturbance caused to the state [26]. Oreshkov and Brun, in 2005, wrote down a weak measurement POVM and showed that any generalized measurement can be decomposed into a sequence of weak measurements, without using an ancilla [27]. Lundeen *et al.* recently came up with a method employing weak values to directly measure the wave function of a quantum system in a pure state [28] and followed it up with a method to measure any general state [29]. For some further developments in this regard, see [30]. Unsharp measurements have also been used to make sequential measurements on a single qubit [6]. Other examples of quantum state tomography with weak measurements can be found in [31–33]. An approach to perform quantum state tomography using weak measurement POVMs was introduced by Hofmann [34].

III. QUANTUM STATE ESTIMATION OF A SINGLE QUBIT

We now turn to the question of using weak measurements with state recycling for the problem of state estimation of a single qubit.

A. The scheme

In our prescription, we consider a finite-size ensemble of pure or mixed states of a qubit. On every member of the ensemble we carry out a σ_z measurement whose strength is defined by the parameter ϵ_1. We record the meter reading in each case and keep the modified states after measurements to obtain a changed ensemble. This new ensemble is now used to measure σ_x in the same way but with a coupling strength ϵ_2. Finally the resultant ensemble is used to carry out projective measurement of σ_y on its members. The first two measurements are weak while the last measurement is strong or projective. To avoid statistical errors the results are averaged over many runs. The entire process is summarized in Fig. 1. For both the weak measurements, consider a regime in which ϵ is neither too large to make the measurement projective, nor too small, as is done in traditional weak measurements. For such

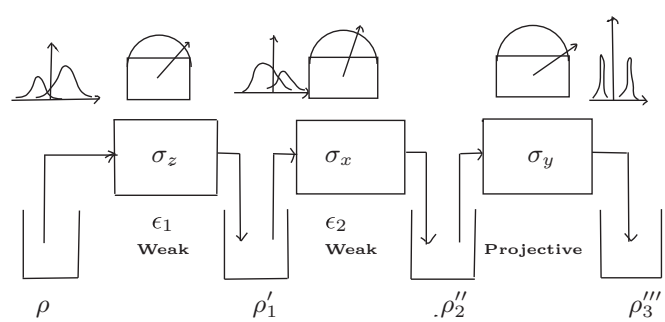

FIG. 1. The schematic diagram of our scheme where we pick a copy of the qubit in state ρ from the first box and perform the measurement of σ_z weakly defined through the system apparatus coupling strength ϵ_1. The state after this measurement changes to ρ_1', on which we perform the measurement of σ_x again weakly defined through the coupling strength ϵ_2. The state now changes to ρ_2'' on which we perform a projective measurement of σ_y. The state after the projective measurement is ρ_3''' and we discard this copy since no information can be extracted from the ensemble. The overlapping Gaussians in the first two cases indicate that the measurement is weak while the nonoverlapping outcomes in the last case indicate that the measurement is projective in nature.

values of ϵ, the two Gaussians, representing the pointer value distributions for the two eigenvalues of the observable, overlap partially with each other. When there is no overlap, a meter reading unambiguously indicates an outcome and we have a projective measurement. A meter reading corresponding to a point in the overlap region cannot be reliably correlated with the system being in one or the other eigenstate. To reduce this difficulty, let us define a region, midway between the centers of the two Gaussians, of width $2a$. We call it the discard region, which means that any pointer reading which falls in this region is rejected. For the case where we measure σ_z, all readings where the pointer position is to the right of this region are interpreted as indicating the value of σ_z to be $+1$ while the ones on the left of this region are interpreted as -1. Even when the outcome is discarded, the member of the ensemble is not rejected, but is retained to be reused for the next measurement. In summary, in this scheme as is shown in Fig. 1 we first measure σ_z weakly, followed by σ_x which is again measured weakly, and last we make a projective measurement of σ_y. The entire simulation is run on identically prepared copies (ensemble size) of the state of interest (pure or mixed). The simulation is repeated many times to avoid statistical errors.

A general single qubit state is given by

$$\rho = \begin{pmatrix} \rho_{00} & \rho_{01} \\ \rho_{10} & \rho_{11} \end{pmatrix} = \rho_{00}|0\rangle\langle 0| + \rho_{01}|0\rangle\langle 1| + \rho_{10}|1\rangle\langle 0| + \rho_{11}|1\rangle\langle 1|. \tag{11}$$

The diagonal elements are known as populations as they give the probabilities with which the states $|0\rangle$ and $|1\rangle$ are present in the mixture. The off-diagonal elements are known as coherences as these contain the phase information of the states $|0\rangle$ and $|1\rangle$. When the state is coupled to a measurement device, as discussed above, the resultant state after unitary evolution for a strength ϵ is

$$\begin{aligned}\rho' = &\left(\frac{\epsilon}{2\pi}\right)^{\frac{1}{2}} \\ &\times\left[\int_{-\infty}^{\infty} dq \int_{-\infty}^{\infty} dq' \rho_{00}\, e^{-\frac{\epsilon(q-1)^2}{4}}\, e^{-\frac{\epsilon(q'-1)^2}{4}} |0\rangle\langle 0| \right. \\ &+ \int_{-\infty}^{\infty} dq \int_{-\infty}^{\infty} dq' \rho_{01}\, e^{-\frac{\epsilon(q-1)^2}{4}}\, e^{-\frac{\epsilon(q'+1)^2}{4}} |0\rangle\langle 1| \\ &+ \int_{-\infty}^{\infty} dq \int_{-\infty}^{\infty} dq' \rho_{10}\, e^{-\frac{\epsilon(q+1)^2}{4}}\, e^{-\frac{\epsilon(q'-1)^2}{4}} |1\rangle\langle 0| \\ &\left. + \int_{-\infty}^{\infty} dq \int_{-\infty}^{\infty} dq' \rho_{11}\, e^{-\frac{\epsilon(q+1)^2}{4}}\, e^{-\frac{\epsilon(q'+1)^2}{4}} |1\rangle\langle 1|\right] \\ &\otimes |q\rangle\langle q'|. \end{aligned} \tag{12}$$

Let us consider taking out a member of the ensemble of system states and then coupling it with the apparatus. Now when the observer notes down the meter reading he or she can see a particular reading which depends upon the initial states of the system and the meter and the coupling between the two. Though this process is not well understood and von Neumann's model is silent about this final step of collapse, it can be thought of as the action of the projector $|q\rangle\langle q|$ on the meter state resulting in the meter reading q.

The probability density of obtaining the value q for the meter is therefore given by

$$P(q) = \mathrm{Tr}(|q\rangle\langle q|\rho_{\mathrm{MD}}), \tag{13}$$

where the reduced density operator for the apparatus or the measuring device (MD) is obtained by taking a partial trace of the state ρ' over the system:

$$\rho_{\mathrm{MD}} = \mathrm{Tr}_{\mathrm{system}}(\rho'). \tag{14}$$

This probability density can now be used to calculate the probabilities of possible outcomes. For example, $P(\sigma_z = 1)$ can be obtained by integrating the probability density from $+a$ to ∞. Thus, the probabilities with which we obtain $+1$, -1, or ambiguous readings while measuring in the z basis are calculated by integrating the above probability densities from $+a$ to ∞, $-\infty$ to $-a$, and $-a$ to $+a$, respectively, and are given by

$$\begin{aligned} P(|0\rangle) &= \frac{1}{4}\left[(1+z)\mathrm{Erfc}\frac{(-1+a)\sqrt{\epsilon_1}}{\sqrt{2}} \right. \\ &\quad \left. -(-1+z)\mathrm{Erfc}\frac{(1+a)\sqrt{\epsilon_1}}{\sqrt{2}}\right], \\ P(|1\rangle) &= \frac{1}{4}\left[-(-1+z)\mathrm{Erfc}\frac{(-1+a)\sqrt{\epsilon_1}}{\sqrt{2}} \right. \\ &\quad \left. +(1+z)\mathrm{Erfc}\frac{(1+a)\sqrt{\epsilon_1}}{\sqrt{2}}\right], \\ P(\mathrm{discard}_z) &= \frac{1}{2}\left[\mathrm{Erf}\frac{(-1+a)\sqrt{\epsilon_1}}{\sqrt{2}} + \mathrm{Erf}\frac{(1+a)\sqrt{\epsilon_1}}{\sqrt{2}}\right]. \end{aligned} \tag{15}$$

Further for the second weak measurement, the input state is the output from the first measurement described by an ensemble ρ_1'. This ensemble is obtained from the state ρ' given in Eq. (12) by taking a trace over the measuring device (apparatus):

$$\rho_1' = \mathrm{Tr}_{\mathrm{MD}}(\rho'). \tag{16}$$

The probabilities with which we obtain the value $+1$, -1, or ambiguous readings while measuring in the σ_x basis are given by

$$\begin{aligned} P(|\sigma_x;+\rangle) &= \frac{1}{4}e^{-\frac{\epsilon_1}{2}}\left[\left(-\mathrm{Erf}(-1+a)\sqrt{\frac{\epsilon_2}{2}} + \mathrm{Erf}(1+a)\sqrt{\frac{\epsilon_2}{2}}\right)x + e^{\frac{\epsilon_1}{2}}\left(\mathrm{Erfc}(-1+a)\sqrt{\frac{\epsilon_2}{2}} + \mathrm{Erfc}(1+a)\sqrt{\frac{\epsilon_2}{2}}\right)\right], \\ P(|\sigma_x;-\rangle) &= \frac{1}{4}e^{-\frac{\epsilon_1}{2}}\left[\left(\mathrm{Erf}(-1+a)\sqrt{\frac{\epsilon_2}{2}} - \mathrm{Erf}(1+a)\sqrt{\frac{\epsilon_2}{2}}\right)x + e^{\frac{\epsilon_1}{2}}\left(\mathrm{Erfc}(-1+a)\sqrt{\frac{\epsilon_2}{2}} + \mathrm{Erfc}(1+a)\sqrt{\frac{\epsilon_2}{2}}\right)\right], \\ P(\mathrm{discard}_x) &= \frac{1}{2}\left[\mathrm{Erf}\frac{(-1+a)\sqrt{\epsilon_1}}{\sqrt{2}} + \mathrm{Erf}\frac{(1+a)\sqrt{\epsilon_1}}{\sqrt{2}}\right]. \end{aligned} \tag{17}$$

After this measurement if we trace over the second apparatus we obtain the ensemble represented through a density operator ρ_2''. Lastly we perform a regular strong (projective) measurement of σ_y and the probabilities are given by

$$\begin{aligned} P(|\sigma_y;+\rangle) &= \tfrac{1}{2}\big[1 + e^{-\frac{1}{2}(\epsilon_1+\epsilon_2)}y\big], \\ P(|\sigma_y;-\rangle) &= \tfrac{1}{2}\big[1 - e^{-\frac{1}{2}(\epsilon_1+\epsilon_2)}y\big]. \end{aligned} \tag{18}$$

In the above equations, we have used

$$\begin{aligned} \mathrm{Erf}(x) &= \frac{2}{\sqrt{\pi}}\int_0^x e^{-t^2}dt, \\ \mathrm{Erfc}(x) &= 1 - \mathrm{Erf}(x). \end{aligned} \tag{19}$$

These measurements when repeated over the entire ensemble give us an estimate of the expectation values of σ_x, σ_y, and σ_z, which in turn help us locate the coordinates (x,y,z) of the point inside the Bloch sphere:

$$\begin{aligned} z &= \mathrm{Tr}(\rho\sigma_z), \\ x &= \mathrm{Tr}(\rho_1'\sigma_x)e^{\frac{\epsilon_1}{2}}, \\ y &= \mathrm{Tr}(\rho_2''\sigma_y)e^{\frac{1}{2}(\epsilon_1+\epsilon_2)}, \end{aligned} \tag{20}$$

where ρ, ρ_1', and ρ_2'' denote the initial state of the system and those after the first and second measurements, respectively. We note that ϵ_1 and ϵ_2 appear in Eq. (20) because we are interested in the expectation values of σ_x, σ_y, and σ_z for the original state ρ of the system. These results are valid only for small values of ϵ_1 and ϵ_2. In subsequent studies we work with the simplification $\epsilon_1 = \epsilon_2 = \epsilon$.

For a scheme based purely on projective measurements, the ensemble is divided into three equal parts and direct measurements of σ_x, σ_y, and σ_z are performed independently.

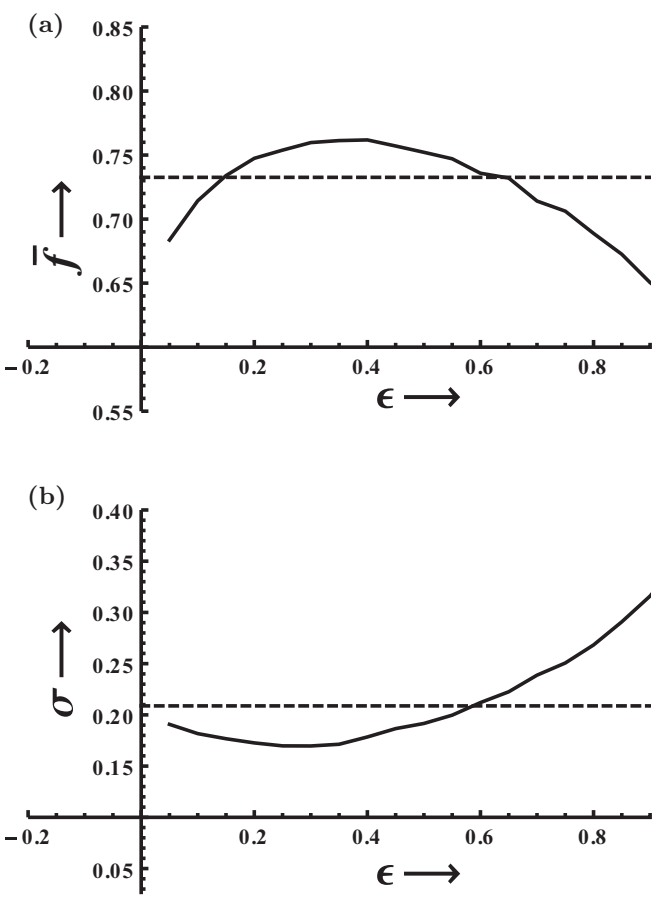

FIG. 2. Fidelity, $\bar{f}$, (a) and standard deviation σ in fidelity (b), plotted as a function of coupling strength ϵ for a randomly chosen state ρ_1. The size of the ensemble here is 30. Weak measurement (solid line) outperforms projective measurement (broken black line) for small ensemble sizes. No values are discarded in this simulation, hence the discard parameter $a = 0$. The straight horizontal dotted line represents the projective measurement and our scheme clearly outperforms the projective measurements.

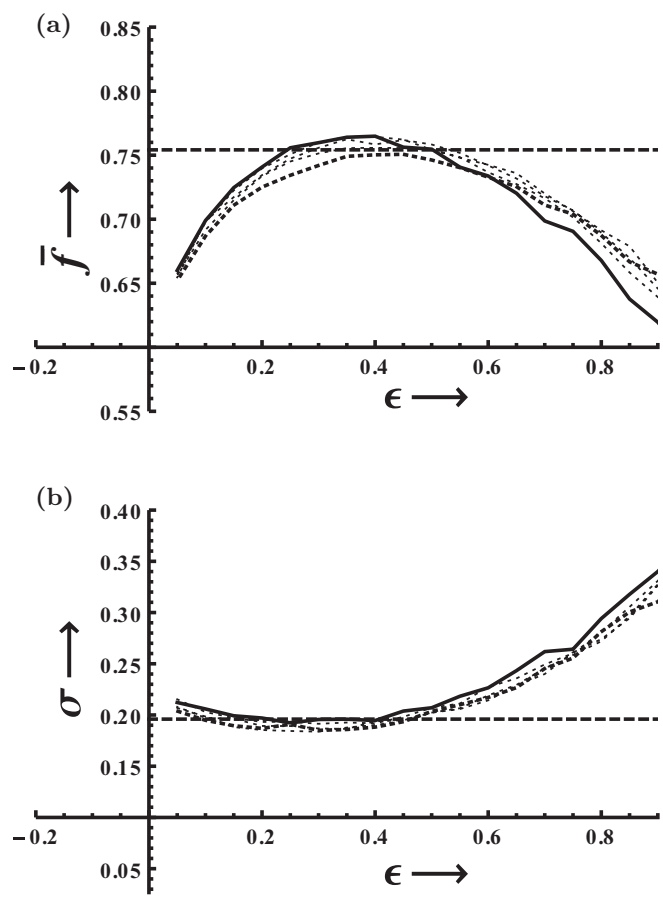

FIG. 3. Fidelities, $\bar{f}$, (a) and standard deviations σ in fidelity (b) plotted as a function of coupling strength ϵ for a randomly chosen state ρ_2 with an ensemble size of 30. In each graph different lines represent different values of the discard parameter a. The discard parameter values plotted are $a = 0$ (dotted thick line), $a = 0.2$ (dotted light line), $a = 0.4$ (dotted light line), $a = 0.6$ (dotted light line), and $a = 0.8$ (solid line). The solid line corresponds to the best case where our scheme outperforms the projective measurements which are represented by the straight horizontal broken line. The standard deviation graph for $a = 0.8$ (the best case) represented by the solid line indicates that the noise in the tomography based on our scheme is not more than that of projective measurements.

This leads to a direct estimate of the expectation values of these operators giving the values of (x,y,z) and hence an estimate of the state. The error in these estimates depends upon the size of the ensemble. We simulate both these schemes and compare the performance of our method with the one based on projective measurements.

B. Two random examples

To begin with we perform the simulations on two randomly generated states ρ_1 and ρ_2 given by

$$\rho_1 = \frac{1}{2}\begin{pmatrix} 1.399 & -0.385+0.042i \\ -0.385-0.042i & 0.601 \end{pmatrix} \tag{21}$$

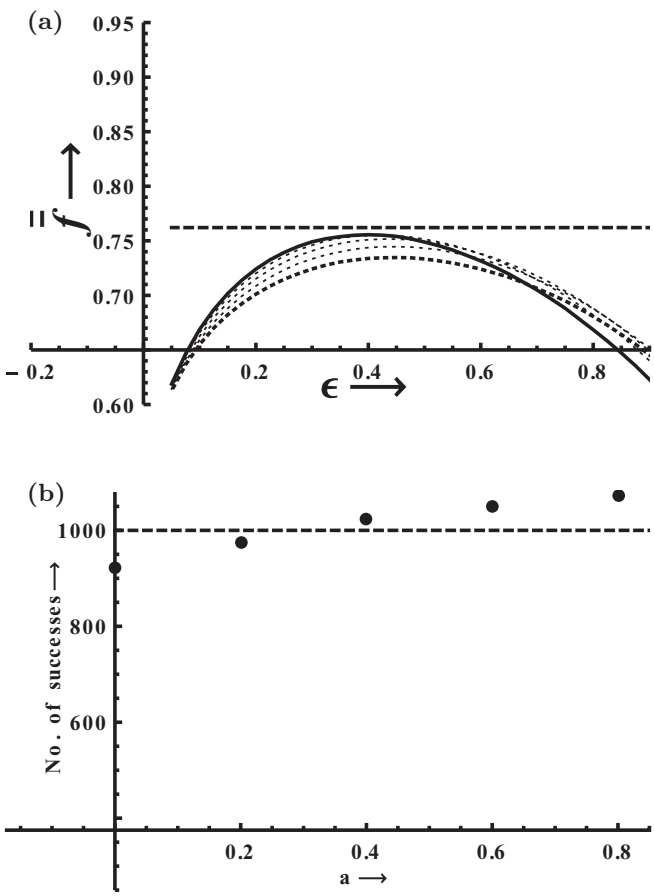

FIG. 4. (a) Plot of the mean fidelity $\bar{\bar{f}}$ for a state with ensemble size 30 and a mean calculated over 1000 runs, further averaged over 2000 randomly chosen states, as a function of the coupling strength ϵ. Different curves represent different values of the discard parameter a. The discard parameters used are $a = 0$ (dotted thick line), $a = 0.2$ (dotted line), $a = 0.4$ (dotted line) $a = 0.6$ (dotted line), and $a = 0.8$ (solid line). The straight dotted line represents projective measurements. The solid line comes very close to the projective measurements. (b) Plot of the number of times our schemes outperform the projective measurement based scheme for the 2000 randomly chosen states of the qubit as a function of the discard parameter a. The dotted horizontal line represents the 50% mark. The performance of our schemes is better than the projective measurement schemes when the discard parameter crosses a certain value (approximately 0.3).

and

$$\rho_2 = \frac{1}{2}\begin{pmatrix} 1.055 & -0.601-0.398i \\ -0.601+0.398i & 0.945 \end{pmatrix}. \tag{22}$$

On the Bloch sphere these states correspond to $(x = -0.385;\ y = -0.042;\ z = 0.397)$ and $(x = -0.601;\ y = 0.398;\ z = 0.055)$, respectively. Both these states are mixed states with distance from the origin of the Bloch sphere for ρ_1 being 0.555 and that for ρ_2 being 0.723. Clearly ρ_2 is less mixed than ρ_1. We would like to stress that these states are randomly chosen.

Taking ensembles of size 30 and putting $\epsilon_1 = \epsilon_2 = \epsilon$ we perform simulations (using Wolfram *Mathematica* 9) over 10 000 runs and calculate the individual fidelity for each run. We use the definition of fidelity defined in Eq. (2). The mean fidelity $\bar{f}$ and the standard deviation σ in fidelity are then plotted as a function of ϵ and in each case a comparison is

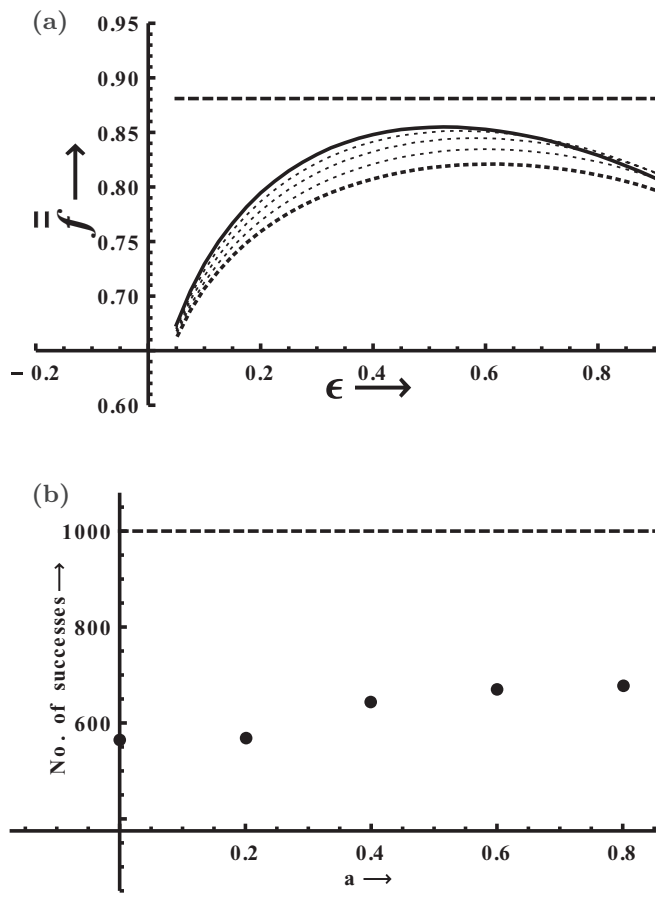

FIG. 5. (a) Plot of the mean fidelity $\bar{\bar{f}}$ for a state with ensemble size 60 and a mean calculated over 1000 runs, further averaged over 2000 randomly chosen states, as a function of the coupling strength ϵ. Different curves represent different values of the discard parameter a. The discard parameters used are $a = 0$ (dotted thick line), $a = 0.2$ (dotted line), $a = 0.4$ (dotted line) $a = 0.6$ (dotted line), and $a = 0.8$ (solid line line). The straight dotted line represents the projective measurements. (b) Plot of the number of times our schemes outperform the projective measurement based scheme for the 2000 randomly chosen states of the qubit as a function of the discard parameter a. The success rate goes down with an increase in ensemble size from 30 to 60.

made with the same parameters for the projective measurement case (see Figs. 2 and 3). We also vary the breadth of the region in which we discard the pointer readings to get an idea of how it affects the quality of state estimation.

In each case we see that there is an interesting dependence of the fidelity of the estimate on ϵ and the discard parameter a. For the case ρ_1 the weak scheme outperforms the projective measurement scheme even without any discard parameter. On the other hand for ρ_2 we have to increase the discard parameter considerably to outperform the projective measurements. However, for another randomly chosen state the scheme may not outperform the projective measurement scheme.

The analysis of the mean fidelity $\bar{f}$ vs ϵ plots shows that there are states such as ρ_1 for which tomography by weak measurements is more effective than projective measurements, for small ensemble sizes (Fig. 2). We note that only in a certain range of ϵ values this is true. The reason is not difficult to see. If ϵ is large then the state of the system is destroyed in the very first measurement of σ_z and the subsequent measurements become meaningless. Again, if ϵ is made too small, then the overlap of the "Gaussians" is too large and a large number of the meter readings fall in the overlapping region. These meter readings then cannot be utilized for any useful purpose under our scheme. The plot of standard deviation in fidelity σ vs ϵ shows that, for the optimal values of ϵ, even the standard deviation of fidelity by weak measurements is less than that for the projective measurements.

There are some states, though, for which this method of estimation does not do better than that by projective measurements. In some of these cases, the estimation can be improved by discarding a certain range of meter readings, as was discussed earlier. The state ρ_2 is an example of such a case where by increasing the discard parameter we can outperform the projective measurements. The results for this state are given in Fig. 3. The average fidelity becomes better than that for the projective measurements and the corresponding standard deviation of fidelity (σ plotted as a function of ϵ) is of the same order as that for projective measurements.

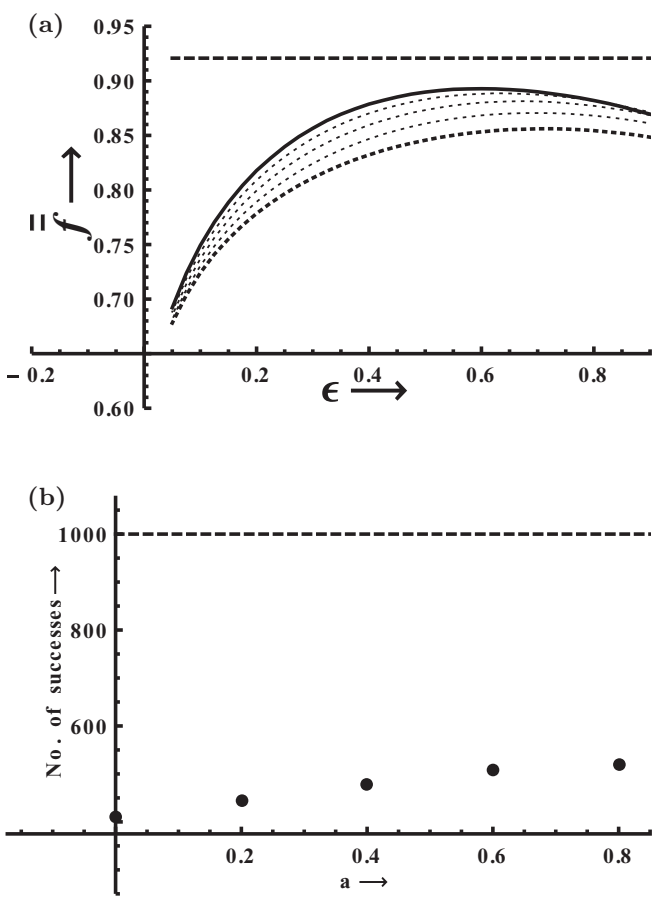

FIG. 6. (a) Plot of the mean fidelity $\bar{\bar{f}}$ for a state with ensemble size 90 and a mean calculated over 1000 runs, further averaged over 2000 randomly chosen states, as a function of the coupling strength ϵ. Different curves represent different values of the discard parameter a. The discard parameters used are $a = 0$ (dotted thick line), $a = 0.2$ (dotted line), $a = 0.4$ (dotted line), $a = 0.6$ (dotted line), and $a = 0.8$ (solid line). The straight dotted line represents the projective measurements. (b) Plot of the number of times our schemes outperform the projective measurement based scheme for the 2000 randomly chosen states of the qubit as a function of the discard parameter a. The success rate further decreases with an increase in ensemble size to 90.

C. Average performance over the Bloch sphere

Encouraged by these results we now move on to test our scheme on a large number of randomly generated states of a qubit and look for the average performance of the scheme over the Bloch sphere. The process is carried out for 2000 states generated randomly. We also study the dependence on ensemble size and use ensemble sizes of 30, 60, and 90. For each case the simulation is repeated 1000 times to average over statistical fluctuations.

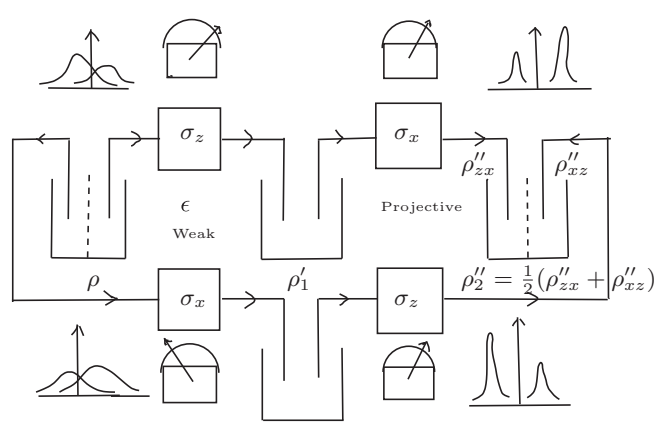

FIG. 7. Block diagram of the weak measurement based state estimation scheme applied to the case when the states lie on a disk in the Bloch sphere with $\langle\sigma_y\rangle = 0$. For such states only two measurements are performed, namely, a weak measurement followed by a projective measurement. To achieve symmetry we divide the ensemble into two halves and for the first half we carry out weak measurement of σ_z followed by a projective measurement of σ_x and for the second half we reverse the order of the measurements. For the first half the final density operator after both the measurements is ρ''_{zx} and the same for the second half is ρ''_{xz}. The density operator for the entire ensemble after the measurement thus is $\rho''_2 = \frac{1}{2}(\rho''_{zx} + \rho''_{xz})$.

While we average the fidelity over all states to obtain the average fidelity we also keep track of whether the scheme outperformed or underperformed as compared to the projective measurement scheme in each case. For the ensemble size of 30, the results of this simulation are presented in two different ways in Fig. 4. We calculate the mean fidelities averaged over these states, $\bar{\bar{f}}$, with and without discard, which are then plotted against ϵ in Fig. 4(a). This graph shows an improvement as we increase the amount of discard. We also present our results through a score plot, where we compute the number of states out of 2000 starting states for which our scheme outperforms the projective measurement scheme. The score plot is described in Fig. 4(b). Interestingly, this number crosses the 50% mark for a threshold value of the discard parameter.

When a study of mean fidelity, averaged over 2000 states, $\bar{\bar{f}}$ vs ϵ, was done, it turns out that although on the average the performance of projective measurements is better, if ambiguous meter readings are discarded, then the number of states for which our tomography scheme is successful goes up. In fact, the number of successes out of 2000 for the discard parameter values of 0, 0.2, 0.4, 0.6, and 0.8 are 923, 973, 1023, 1051, and 1071, respectively. This we think is clear evidence that our scheme has the potential of unearthing more information than projective measurements under certain circumstances. In particular, if we are given 30 copies of an unknown state of a qubit, our scheme will be a better choice for carrying out state tomography.

We now turn to testing our scheme with increasing ensemble size. We repeat the simulation in exactly the same way for the cases of ensemble size 60 and 90. The results are presented in a similar way in Figs. 5 and 6. Increasing the ensemble size clearly reduces the efficacy of our scheme as compared to projective measurements. The score plots show that our scheme outperforms the projective measurement scheme for ensemble sizes of 60 and 90 for a lesser number of states and the number is less than 50%. Therefore we conclude that our scheme is preferable only when we have a small ensemble size. We would like to clarify that this is not due to statistical fluctuations as we have taken the average over a large number of runs even when the ensemble size is small.

D. States with $\langle\sigma_y\rangle = 0$

We now turn to a subset of states in the Bloch sphere, namely, the states with $\langle\sigma_y\rangle = 0$. These states form a disk

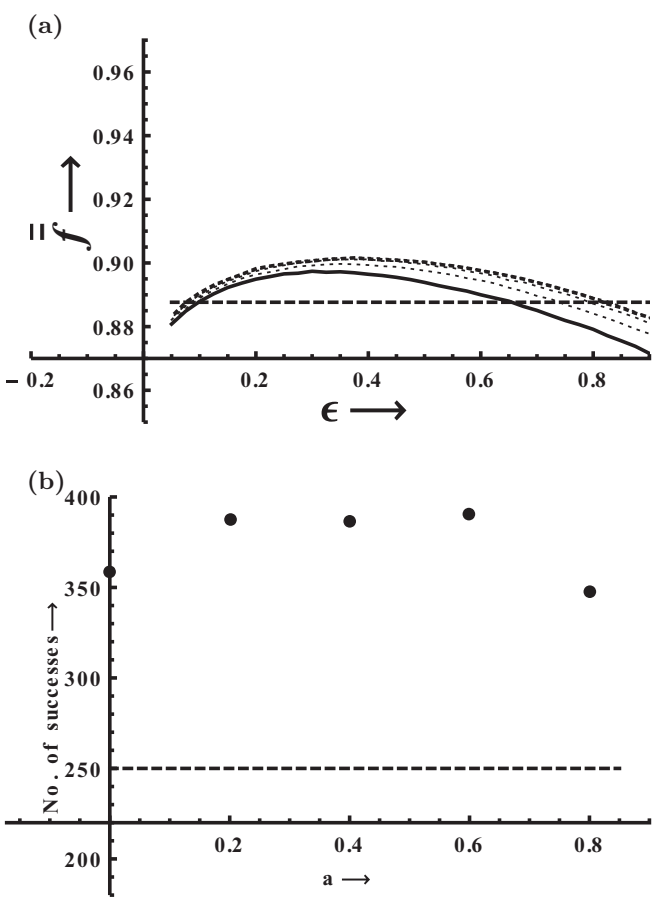

FIG. 8. Results of state estimation for 500 randomly generated states on the disk with $\langle\sigma_y\rangle = 0$ for an ensemble size of 30 with each state averaged over 1000 runs. The average fidelity as a function of ϵ for discard parameter values 0, 0.2, 0.4, 0.6, and 0.8 are shown in part (a). In part (b) the score plot is displayed where we plot the number of successes out of 500 as a function of discard parameter a.

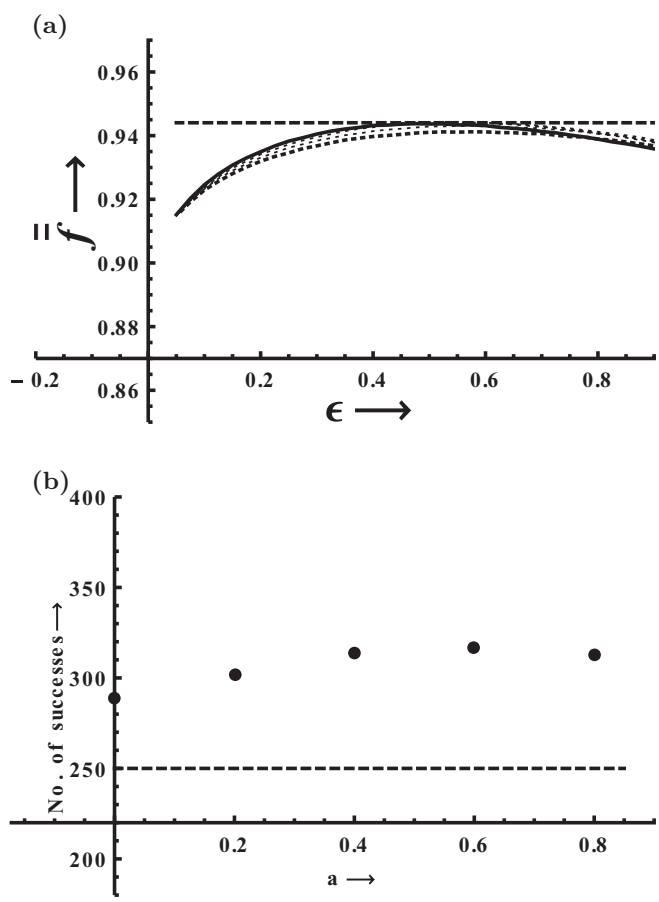

FIG. 9. Results of state estimation for 500 randomly generated states on the disk with $\langle\sigma_y\rangle = 0$ for an ensemble size of 60 with each state averaged over 1000 runs. The average fidelity as a function of ϵ for discard parameter values 0, 0.2, 0.4, 0.6, and 0.8 are shown in part (a). In part (b) the score plot is displayed where we plot the number of successes out of 500 as a function of discard parameter a.

perpendicular to the $\hat{y}$ axis and passing through the origin. The set contains pure states which lie on a circle and mixed states all the way to maximally mixed states which lie in the interior of the disk. Once it is known that a state belongs to this set, estimations of only two parameters are required to know the state. This can be achieved by measuring $\langle\sigma_x\rangle$ and $\langle\sigma_z\rangle$. Given a finite-size ensemble of identically prepared states belonging to this set, how do we estimate the state and how well can we do it? If we employ projective measurements we can divide the ensemble into two equal parts and measure $\langle\sigma_x\rangle$ on one half of the system and measure $\langle\sigma_z\rangle$ on the other half. In our weak measurement based scheme with state recycling, we again divide the ensemble into two equal parts. On the first half we carry out a weak measurement of σ_x of strength ϵ followed by a projective measurement of σ_z while on the second half we reverse the order where we carry out a weak measurement of σ_z followed by a projective measurement of σ_x. The flowchart of this measurement scheme is shown in Fig. 7.

While simulating the scheme, we choose ensemble sizes of 30, 60, and 90 and compare the state estimation efficacy of our scheme with the projective measurement scheme. For each ensemble size, we generate 500 random states in the set and repeat the estimation 1000 times for each state. The results for ensemble size 30 are displayed in Fig. 8. The results are presented exactly in the same way as we did in the previous section. The results of ensemble sizes 60 and 90 are presented in Figs. 9 and 10, respectively.

For this subset of states the weak measurement based scheme does much better. The score plots show that the scheme outperforms the projective measurements in all three cases. The relative efficacy reduces as the ensemble size is increased.

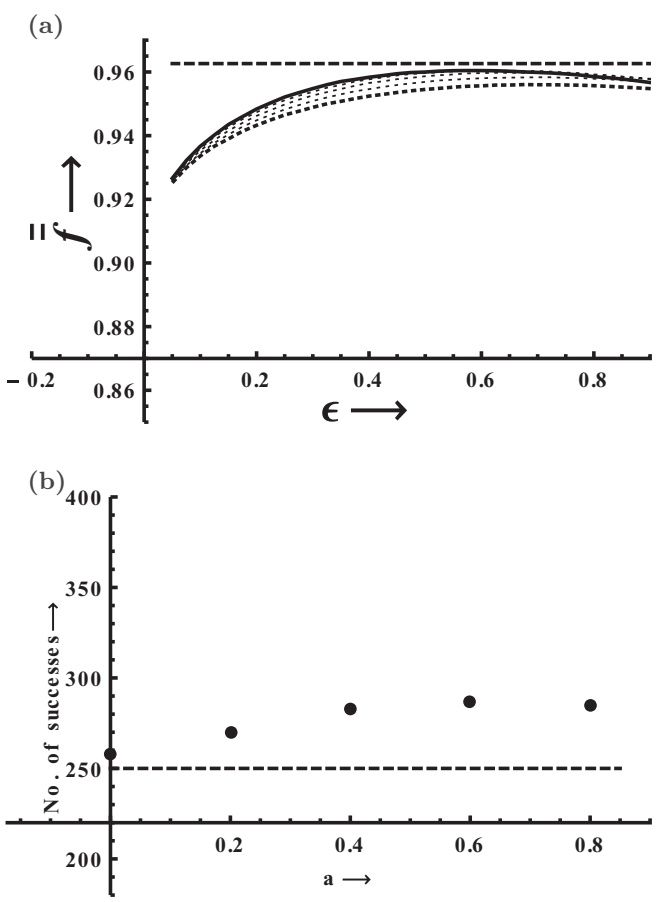

FIG. 10. Results of state estimation for 500 randomly generated states on the disk with $\langle\sigma_y\rangle = 0$ for an ensemble size of 90 with each state averaged over 1000 runs. The average fidelity as a function of ϵ for discard parameter values 0, 0.2, 0.4, 0.6, and 0.8 are shown in part (a). In part (b) the score plot is displayed where we plot the number of successes out of 500 as a function of discard parameter a.

IV. CONCLUDING REMARKS

In this work we have used weak measurements to carry out quantum state tomography on finite-sized (pure or mixed) one-qubit ensembles. We have shown that in such schemes, recycling of states is possible, where one makes more than one measurement on a single copy before discarding a given member of the ensemble of identically prepared states. In general when coupling strengths are small, the pointer positions may overlap, making the outcome of the measurement ambiguous. We have introduced a discard parameter such that the outcomes with most ambiguity are discarded. We have carried out an optimization of the scheme to improve its efficacy with respect to the coupling strength ϵ and the discard parameter a.

Over a randomly chosen subset of qubit states, our scheme performs better than the scheme based on projective measurements. We demonstrate this by showing that the weak measurement based scheme works better for more than 50% of the randomly chosen cases for small ensemble sizes. For a subset of states on the Bloch sphere where we take a disk with $\langle\sigma_y\rangle = 0$ the scheme does very well and is almost always preferable over projective measurements. As the ensemble size increases the relative efficacy of our scheme decreases as seen in the comparative results for varying ensemble sizes.

It is true that an experimenter will not know *a priori* whether, for a given unknown state, which scheme out of projective measurement and weak measurement will be more suitable. However, the experimenter will be able to make an informed choice, depending on knowledge about the ensemble size. In the particular case where the σ_y polarization is zero or for that matter any particular polarization is known to be zero, our method will be a better choice for state estimation.

This has opened up an interesting possibility of estimating quantum states and extracting information from quantum ensembles using weak measurements. We would also like to mention that the original context in which the weak measurements were introduced was related to weak value and postselection. However, we do not carry out any postselection and do not use the weak value. We only use the weak nature of the measurement to recycle the states.

In many physical situations, the apparatus is weakly coupled with the system and hence our scheme may find a natural application for such measurements. In another direction, a natural extension of this scheme on two qubits, where entangled states are possible, can lead to interesting possibilities. In particular, one may be able to detect quantum entanglement by such schemes. A more detailed discussion of this and related results will be taken up elsewhere.

[1] P. Busch and P. J. Lahti, Phys. Rev. D **29**, 1634 (1984).
[2] K. Kraus, A. Böhm, J. D. Dollard, and W. Wootters, in *States, Effects, and Operations Fundamental Notions of Quantum Theory* (Springer, Berlin, Heidelberg, 1983), Vol. 190.
[3] S. T. Ali and G. G. Emch, J. Math. Phys. **15**, 176 (1974).
[4] E. Prugovecki, J. Math. Phys. **17**, 1673 (1976).
[5] S. T. Ali and E. Prugovecki, J. Math. Phys. **18**, 219 (1977).
[6] L. Disi, Fortschr. Phys. **51**, 96 (2003).
[7] T. A. Brun, Am. J. Phys. **70**, 719 (2002).
[8] Y. Aharonov, D. Z. Albert, and L. Vaidman, Phys. Rev. Lett. **60**, 1351 (1988).
[9] I. M. Duck, P. M. Stevenson, and E. C. G. Sudarshan, Phys. Rev. D **40**, 2112 (1989).
[10] Y. Aharonov, S. Popescu, and J. Tollaksen, Phys. Today **63**, 27 (2010).
[11] R. Jozsa, Phys. Rev. A **76**, 044103 (2007).
[12] J. Combes, C. Ferrie, Z. Jiang, and C. M. Caves, Phys. Rev. A **89**, 052117 (2014).
[13] C. Ferrie and J. Combes, Phys. Rev. Lett. **112**, 040406 (2014).
[14] M. A. Nielsen and I. L. Chuang, *Quantum Computation and Quantum Information* (Cambridge University Press, Cambridge, UK, 2000), pp. xxvi+676.
[15] A. Peres, *Quantum Theory: Concepts and Methods*, Fundamental Theories of Physics, Vol. 57 (Kluwer Academic Publishers Group, Dordrecht, 1993).
[16] S. Massar and S. Popescu, Phys. Rev. Lett. **74**, 1259 (1995).
[17] M. Ueda and M. Kitagawa, Phys. Rev. Lett. **68**, 3424 (1992).
[18] C. Branciard, Proc. Natl. Acad. Sci. U.S.A. **110**, 6742 (2013).
[19] Y. W. Cheong and S.-W. Lee, Phys. Rev. Lett. **109**, 150402 (2012).
[20] J. J. Sakurai, *Modern Quantum Mechanics (Revised Edition)* (Addison-Wesley, Reading, MA, 1993).
[21] J. V. Neumann, *Mathematical Foundations of Quantum Mechanics* (Princeton University Press, Princeton, NJ, 1955).
[22] S. Marcovitch and B. Reznik, arXiv:1005.3236.
[23] M. E. Goggin, M. P. Almeida, M. Barbieri, B. P. Lanyon, J. L. OBrien, A. G. White, and G. J. Pryde, Proc. Natl. Acad. Sci. U.S.A., http://www.pnas.org/content/early/2011/01/04/1005774108.abstract.
[24] U. Singh and A. K. Pati, Ann. Phys. **343**, 141 (2014).
[25] U. Singh and A. K. Pati, arXiv:1305.4393.
[26] L. A. Rozema, A. Darabi, D. H. Mahler, A. Hayat, Y. Soudagar, and A. M. Steinberg, Phys. Rev. Lett. **109**, 100404 (2012).
[27] O. Oreshkov and T. A. Brun, Phys. Rev. Lett. **95**, 110409 (2005).
[28] J. S. Lundeen, B. Sutherland, A. Patel, C. Stewart, and C. Bamber, Nature **474**, 188 (2011).
[29] J. S. Lundeen and C. Bamber, Phys. Rev. Lett. **108**, 070402 (2012).
[30] H. F. Hofmann, arXiv:1311.0093.
[31] S. Wu, Sci. Rep. **3**, 1193 (2013).
[32] Y. Shikano and S. Tanaka, Europhys. Lett. **96**, 40002 (2011).
[33] H. Kobayashi, K. Nonaka, and Y. Shikano, Phys. Rev. A **89**, 053816 (2014).
[34] H. F. Hofmann, Phys. Rev. A **81**, 012103 (2010).